

Effect of dark soliton on the spectral evolution of bright soliton in a silicon-on-insulator waveguide

Zhen Liu(刘振), Wei-Guo Jia(贾维国), Hong-Yu Wang(王红玉), Yang Wang(汪洋), Neimule Men-Ke(门克内木乐), Jun-Ping Zhang(张俊萍)

Citation: Chin. Phys. B . 2020, 29(6): 064212 . **doi:** 10.1088/1674-1056/ab84d9
Journal homepage: http://cpb.iphy.ac.cn; http://iopscience.iop.org/cpb

What follows is a list of articles you may be interested in

Soliton evolution and control in a two-mode fiber with two-photon absorption

Qianying Li(李倩颖)

Chin. Phys. B . 2020, 29(1): 014204 . **doi:** 10.1088/1674-1056/ab5784

Propagation characteristics of parallel dark solitons in silicon-on-insulator waveguide

Zhen Liu(刘振), Weiguo Jia(贾维国), Yang Wang(汪洋), Hongyu Wang(王红玉), Neimule Men-Ke(门克内木乐), Jun-Ping Zhang(张俊萍)

Chin. Phys. B . 2020, 29(1): 014203 . **doi:** 10.1088/1674-1056/ab577d

Soliton guidance and nonlinear coupling for polarized vector spiraling elliptic Hermite-Gaussian beams in nonlocal nonlinear media

Chunzhi Sun(孙春志), Guo Liang(梁果)

Chin. Phys. B . 2019, 28(7): 074206 . **doi:** 10.1088/1674-1056/28/7/074206

Nonlinear effect of the structured light profilometry in the phase-shifting method and error correction

Zhang Wan-Zhen, Chen Zhe-Bo, Xia Bin-Feng, Lin Bin, Cao Xiang-Qun

Chin. Phys. B . 2014, 23(4): 044212 . **doi:** 10.1088/1674-1056/23/4/044212

Mid-IR dual-wavelength difference frequency generation in uniform grating PPLN using index dispersion control

Chang Jian-Hua, Sun Qing, Ge Yi-Xian, Wang Ting-Ting, Tao Zai-Hong, Zhang Chuang

Chin. Phys. B . 2013, 22(12): 124204 . **doi:** 10.1088/1674-1056/22/12/124204

Effect of dark soliton on the spectral evolution of bright soliton in a silicon-on-insulator waveguide*

Zhen Liu(刘振), Wei-Guo Jia(贾维国)†, Hong-Yu Wang(王红玉), Yang Wang(汪洋), Neimule Men-Ke(门克内木乐), and Jun-Ping Zhang(张俊萍)

School of Physical Science and Technology, Inner Mongolia University, Hohhot 010021, *China*

(Received 15 February 2020; revised manuscript received 11 March 2020; accepted manuscript online 31 March 2020)

The spectral evolution of bright soliton in a silicon-on-insulator optical waveguide is numerically simulated using the split-step Fourier method. The power and input chirp of the dark soliton and the second-order dispersion are varied to investigate the effect of dark soliton on the spectrum of bright soliton. The simulations prove that the dark soliton modifies the spectral shape of the bright soliton. Further, the variation in the power of dark soliton affects the splitting of bright soliton. Furthermore, the chirped dark soliton can improve the spectral width and flatness. The variation in the dispersion of dark soliton modifies the phase matching of the bright soliton and the dispersive wave emission, thereby affecting the spectral evolution.

Keywords: spectral evolution, silicon-based optical waveguide, nonlinear effect, bright and dark solitons, phase matching

PACS: 42.65.Tg, 42.65.–k, 73.40.Qv, 42.25.Bs **DOI:** 10.1088/1674-1056/ab84d9

1. Introduction

An optical spectrum encompasses a series of electromagnetic waves arranged according to wavelength or frequency, which is formed due to the dispersion of polychromatic light through a dispersive system.[1] Spectral analysis is applied in a variety of fields such as hyperspectral remote sensing,[2] optical frequency comb,[3] spectral mask,[4] *etc*. With recent breakthroughs, spectrometers have been miniaturized to nano-scales,[5] among which the near-infrared[6] and Raman[7] spectrometers are widely used to explore the structure and chemical composition of substances.

The spectrum of the bright solitons represents the variation in the energy states of photons.[1] Therefore, the free carriers induced by two-photon absorption in silicon-based optical waveguides affects the width and flatness of the soliton spectrum. To this end, ridge waveguides allow a quicker dissipation of free carriers[8] and can avoid the effect of free-carrier overload. In optical waveguides, self-phase modulation,[9] soliton splitting,[10] dispersive wave generation,[11] and input chirps[12] have a significant impact on the spectral evolution. In contrast, higher-order Raman effect and self-steepening effect have a minor effect on the spectral lines. In the time domain, when a dark soliton is simultaneously input with the bright soliton, it significantly impacts the pulse morphology, peak value, and effective propagation distance of the bright soliton,[13] thus affecting its spectral evolution. In this study, the spectral morphology of the bright soliton accompanied by dark soliton is numerically simulated by a MATLAB program. Further, the effect of the power, input chirp, and dispersion intensity of the dark soliton on the spectrum of the bright soliton is investigated.

2. Theoretical model

In birefringent silicon-based optical waveguide (SOI), the pulse transmission can be obtained in terms of coupled nonlinear Schrödinger equations as follows:[14–16]

$$\begin{aligned}&\frac{\partial A_x}{\partial z}+\delta\frac{\partial A_x}{\partial T}+\frac{\mathrm{i}}{2}\beta_{2x}\frac{\partial^2 A_x}{\partial T^2}-\frac{1}{6}\beta_{3x}\frac{\partial^3 A_x}{\partial T^3}\\ &=-\frac{1}{2}(\alpha_{\mathrm{l}}+\alpha_{\mathrm{fc}})A_x+\mathrm{i}k_0 n_{\mathrm{fc}}A_x\\ &\quad+\mathrm{i}\gamma\left(1+\frac{\mathrm{i}}{\omega_0}\frac{\partial}{\partial T}\right)\left(\frac{1+\rho}{2}|A_x|^2+\frac{2\rho}{3}|A_y|^2\right)A_x, \quad (1a)\\ &\frac{\partial A_y}{\partial z}+\delta\frac{\partial A_y}{\partial T}+\frac{\mathrm{i}}{2}\beta_{2y}\frac{\partial^2 A_y}{\partial T^2}-\frac{1}{6}\beta_{3y}\frac{\partial^3 A_y}{\partial T^3}\\ &=-\frac{1}{2}(\alpha_{\mathrm{l}}+\alpha_{\mathrm{fc}})A_y+\mathrm{i}k_0 n_{\mathrm{fc}}A_y\\ &\quad+\mathrm{i}\gamma\left(1+\frac{\mathrm{i}}{\omega_0}\frac{\partial}{\partial T}\right)\left(|A_y|^2+\frac{2\rho}{3}|A_x|^2\right)A_y. \quad (1b)\end{aligned}$$

Here, A_x and A_y are two slow-varying envelope amplitudes that are perpendicular to each other. A_x and A_y correspond to the normal and anomalous dispersion regions, respectively. β_{2x}, β_{2y}, β_{3x}, and β_{3y} represent the second- and third-order dispersions in two polarization directions, z is the transmission distance, T is the time parameter under the reference frame of group velocity, δ is the detuning, ω_0 is the angular frequency

*Project supported by the National Natural Science Foundation of China (Grant No. 61741509).

†Corresponding author. E-mail: jwg1960@163.com

© 2020 Chinese Physical Society and IOP Publishing Ltd

of the pulse, α_l is the linear loss coefficient with a numerical value of 0.2 dB/cm, and α_{fc} is the free-carrier loss coefficient, which can be obtained using $\alpha_{fc} = \sigma N_C$, where $\sigma \approx 1.45 \times 10^{-21}$ m^2 is the free-carrier absorption coefficient. n_{fc} is the change in refractive index caused by a free carrier, which can be obtained as $n_{fc} = 2k_c N_C$, and $k_c = 1.35 \times 10^{-27}$ m is the wavenumber of the free carrier. N_C is the average free-carrier concentration generated by two-photon absorption, whose evolution can be expressed as follows:[17]

$$\frac{dN_C(z,T)}{dt} = \frac{\beta_{TPA}}{2h\nu_0 A_{eff}^2}|A(z,T)|^4 - \frac{N_C(z,T)}{\tau_{eff}}, \quad (2)$$

where h is the Planck constant, ν_0 is the photon frequency, β_{TPA} is the two-photon absorption coefficient, A_{eff} is the effective module area, $A(zT)$ is the total field distribution, and τ_{eff} is the free carrier lifetime. In Eq. (1), γ is the nonlinear coefficient obtained from $\gamma = n_2 k_0/A_{eff} + i\beta_{TPA}/A_{eff}$, where $n_2 \approx 6 \times 10^{-18}$ m^2/W is the Kerr coefficient. The higher order solitons satisfy the following equation: $N^2 = \mathrm{Re}(\gamma)P_0 T_0^2/\beta_2$. The order of solitons affect the splitting effect and dispersive wave generation. The phase matching condition for the generation of dispersive wave radiation is[18]

$$\sum_{m\geqslant 2} \frac{\beta_n(\omega_s)}{m!}(\omega_R - \omega_s)^m = \frac{\gamma_0(\omega_s)P_0}{2},$$

where ω_R and ω_s are the angular frequencies of dispersive wave and transmitted soliton, respectively, and γ_0 is the nonlinear coefficient calculated at ω_s.

Kerr effect and two-photon absorption are the primary nonlinear effects in a waveguide. Because the pulse width is assumed to be larger than 100 fs, dispersion above the third order and the self-steepening effect of the Raman scattering are not considered. The parameter ρ represents the material property of silicon, and its numerical value is 1.27.

3. Numerical analysis

We implemented SOI ridge waveguide for numerical simulation. A schematic diagram of the waveguide structure is shown in Fig. 1. The incident light propagates along the Z axis of the waveguide, and it is polarized along the X-axis direction, which corresponds to the normal dispersion region that allows the entry of the dark soliton A_x. Further, the Y-axis direction corresponds to the anomalous dispersion region that facilitates the entry of the bright soliton A_y. To ensure the accuracy of simulation, we selected the following parameters for the waveguide: length $L = 5$ mm, width $W = 1$ μm, height $H = 0.6$ μm, and etching depth $h = 0.3$ μm. The initial input pulse comprised of bright and dark soliton pulse with input wavelength of 1550 nm and pulse width of 250 fs.

The two-pulse envelope waveform can be expressed as follows:

$$A_x = \sqrt{P_1}\tanh(T/T_0)\exp\left(\frac{-iCT^2}{2T_0^2}\right),$$
$$A_y = \sqrt{P_2}\,\mathrm{sech}(T/T_0),$$

where $P_1 = P_2 = 20$ W is the power of the two input pulses, T_0 is the pulse width, and C is the chirp parameter of the soliton. The setting parameters are as follows: $\beta_{2x} = 30$ ps^2/m, $\beta_{2y} = -10$ ps^2/m, $\beta_{3x} = 0.6$ ps^3/m, and $\beta_{3y} = 1$ ps^3/m. The group refractive indices are $n_x = 3.3$ and $n_y = 3.2$.

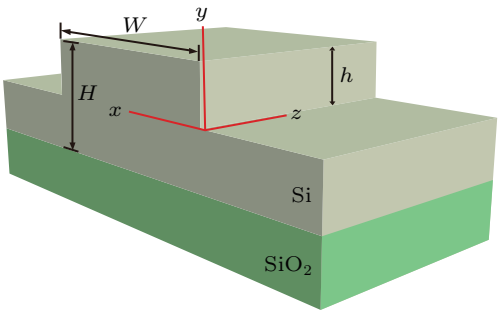


Fig. 1. Schematic diagram of the SOI optical waveguide structure.

To explore the influence of dark solitons on the spectral evolution of bright solitons in ridged silicon-based optical waveguides, we compared the transmission of bright solitons in the presence and absence of dark solitons. The simulated diagram for spectral evolution is shown in Fig. 2.

It is evident from Figs. 2(a) and 2(c) that there is only one main peak in the first 5 mm of the single bright-soliton spectrum, which exhibits high intensity and small fluctuation. However, as the transmission distance increases, this peak is broadened and exhibits a blueshift due to self-phase modulation. Above 5 mm, the spectrum is split into two parts, as shown in Fig. 2(c). The left part comprises a continuous spectrum with small intensity caused by soliton splitting, and the raised structure corresponds to the dispersive wave radiation.[19] The peak at the right is similar to that in the input spectrum. The addition of the dark soliton polarized in the X direction has a considerable effect on the spectral evolution of the bright soliton. Figures 2(b) and 2(d) show that the spectral width is almost unchanged for the first 5 mm with a slight blueshift. After 5 mm, the peak intensity in the redshift direction increases with the transmission distance. After 10 mm, a continuous spectrum is observed in the blueshift direction due to the splitting of solitons, and a vibrating structure is observed in the redshift direction, which significantly broadens the spectrum. Figure 2(d) shows that the bright soliton fails to generate a dispersive wave under the effect of dark soliton. To encapsulate, the dark soliton considerably affects the spectral evolution of bright soliton, where the splitting of the soliton is reduced and the phase mismatch of the bright soliton cannot generate dispersive wave radiation.

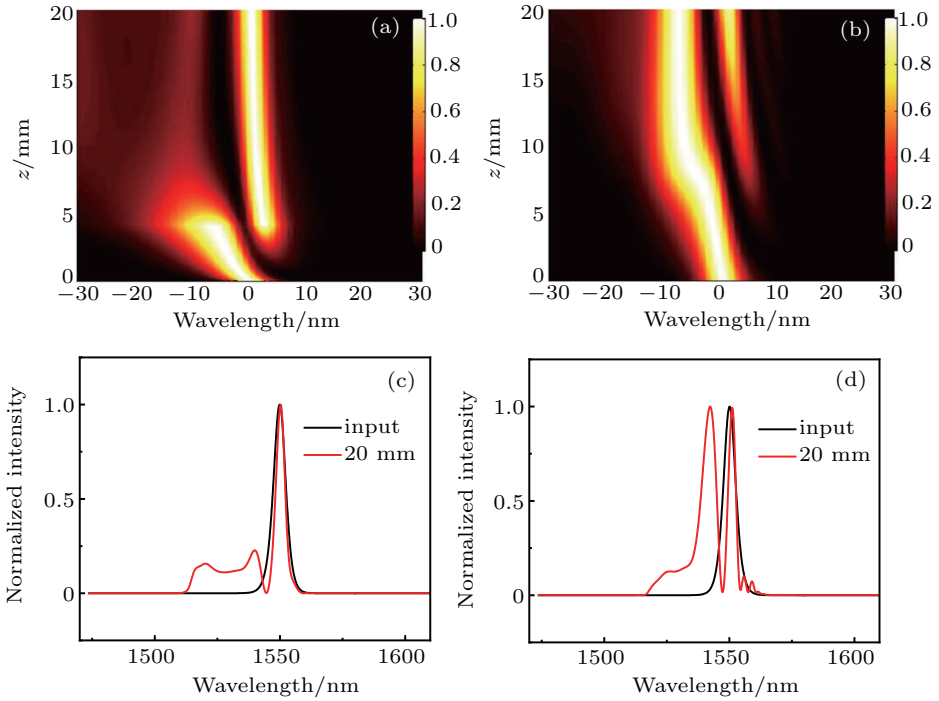


Fig. 2. Evolution diagram and spectral line distribution of bright soliton in ridge SOI under different conditions. Spectral evolution diagram for (a) bright soliton only and (b) bright soliton under the influence of dark soliton. Input and output spectral lines for (c) bright soliton only and (d) bright soliton under the influence of dark soliton.

3.1. Effect of soliton power

We varied the power of the soliton to investigate the effect of soliton splitting, *i.e.*, the order of soliton on the spectrum of the bright soliton. Initially, the power of the bright soliton was kept constant at 20 W, and the power of the dark soliton was varied as 20 W, 40 W, and 60 W. Subsequently, the power of the bright soliton was changed to 40 W and 60 W, and the spectral evolution of the bright soliton under the nine power combinations was simulated.

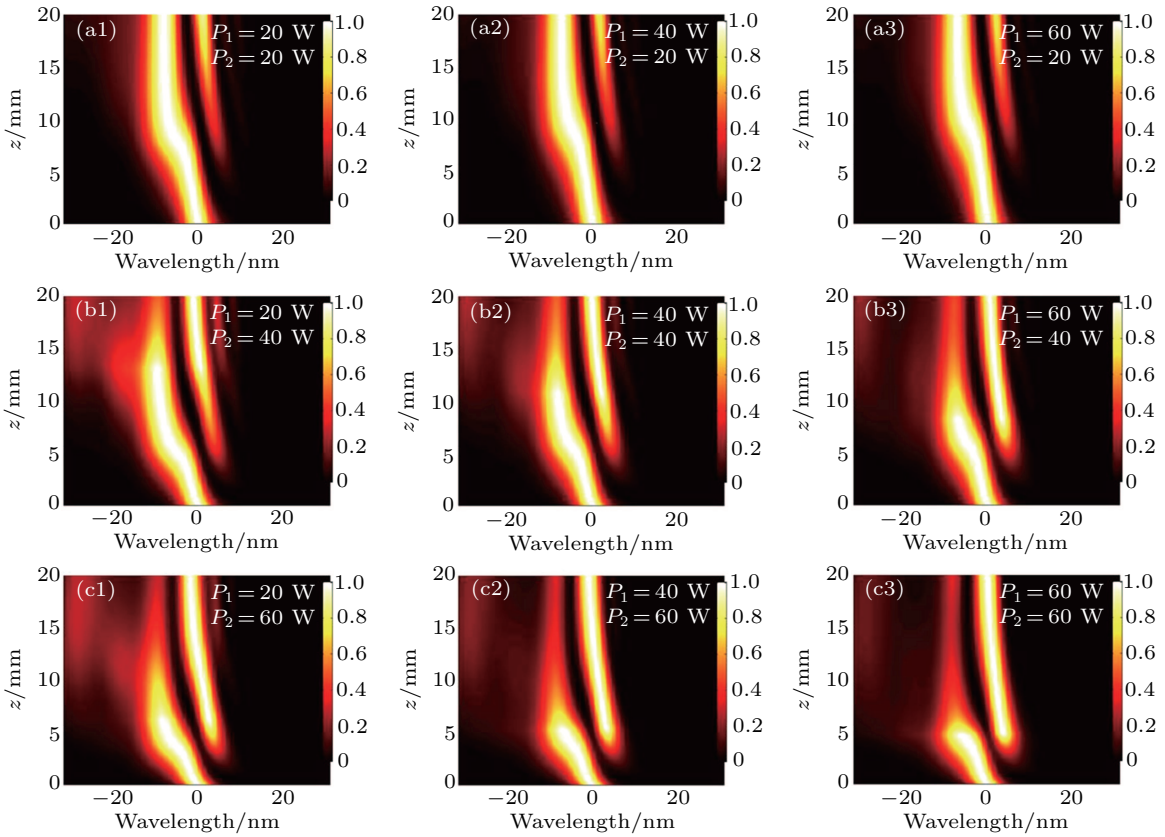


Fig. 3. Spectral evolution of bright soliton at different powers of bright and dark solitons. Here, P_1 is varied. (a) $P_2 = 20$ W, (b) $P_2 = 40$ W, and (c) $P_2 = 60$ W.

Figures 3(a) and 4(a) show that the spectral evolution of the bright soliton basically remains unchanged when the power of the bright soliton is 20 W and that of the dark soliton is increased. Only a slight decrease is observed for the amplitude of the blue-shifted part in the continuous structure and for the peak position of the red-shifted structure on the right. It is clear from Figs. 3(b) and 4(b) that spectrum is significantly changed when the power of bright soliton is increased to 40 W. The splitting of the soliton becomes more prominent, and a continuous spectrum is observed in the blueshift direction. When the power of the dark soliton is increased, the continuous spectrum is generated earlier, and the whole spectrum is broadened. The dispersive wave radiation is generated at the wavelength of 1520 nm, and the bulge of the radiation structure is more obvious due to the increase in the power of dark soliton. On the right side of the spectrum, an oscillating structure is still observed. As P_1 increases, the oscillating structure appears later, and the oscillation amplitude decreases. As shown in Figs. 3(c) and 4(c), when the power of the bright soliton is increased to 60 W, the flatness and expansion of the continuous spectrum on the left increase as compared to that in the spectrum with $P_2 = 40$ W. As P_1 increases, the dispersive wave radiation gradually fails to meet the conditions, and the convex structure disappears. As the power of the dark soliton is increased, the oscillating structure in the redshift direction appears later. Finally, when the power of both bright and dark solitons is 60 W, the oscillating structure completely disappears, and the entire spectrum is similar to that obtained when the bright soliton is transmitted alone. Therefore, when the energy of the dark soliton is high, the energy of the bright soliton energy is affected, which influences the splitting of bright soliton and promotes the phase matching. When the energy of both bright and dark solitons is high, the spectrum of bright soliton ceases to be affected by the dark soliton.

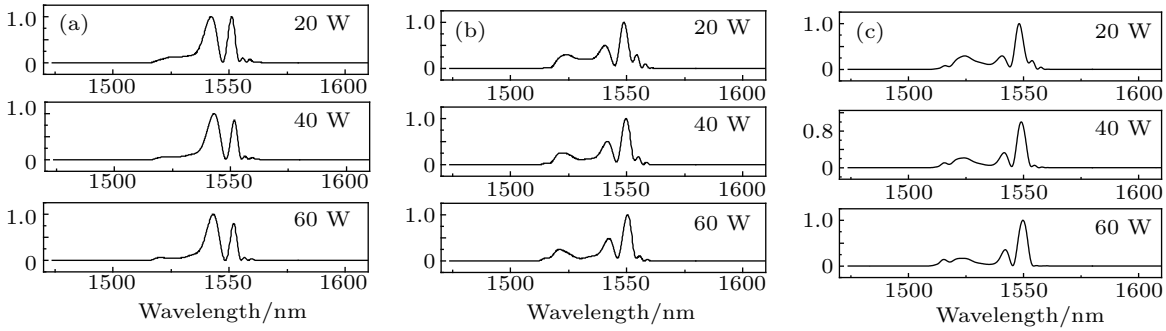


Fig. 4. Spectral lines of bright soliton at different powers of bright and dark solitons at 20 mm. Here, P_1 is varied. (a) $P_2 = 20$ W, (b) $P_2 = 40$ W, and (c) $P_2 = 60$ W.

3.2. Effect of chirp

Most of the femtosecond pulses generated in lasers are chirped. For exploring the effect of chirped dark soliton on the spectrum of bright soliton, we varied the chirped parameter C of dark soliton while keeping the power of bright and dark soliton as 20 W.

Figure 5 shows that when the chirped dark soliton and bright soliton are input at the same time, the continuous structure on the left side of the bright soliton spectrum disappears, indicating that the dark soliton can inhibit the splitting of bright soliton. The spectrum is modified with the increase in the chirp coefficient. In the evolution process, the spectrum with a blueshift trend gradually becomes symmetric due to self-phase modulation, presenting the evolutionary shape in Fig. 5(a4). Figure 5(b) shows that as the chirp of dark soliton (C) increases, the peak in the redshift direction gradually rises with the increase of transmission distance. By comparing the four spectra with different values of C, it can be observed that the peak value of the right peak is enlarged with the increase of C. For $C = 0.9$, it exceeds the peak value at 1550 nm. When $C > 0.6$, the spectrum is no longer blue-shifted and a flat undulation structure appears in the blueshift direction. As C increases, the undulation structure appears earlier and lasts longer. Therefore, the chirped dark soliton effectively enhances the self-phase modulation in waveguides and suppresses the splitting of solitons, so that the flatness and width of the entire spectrum can be optimized.

Figure 6 shows when a negative chirp is introduced into the dark soliton, the most obvious characteristic of the bright soliton spectrum is that a truncation point appears in the evolution process. The spectral line at the truncation point protrudes from the evolutionary graph and truncates the original evolutionary graph due to blueshift. Moreover, the truncation point appears earlier if C decreases. The continuous spectrum in the blueshift direction caused by the splitting of soliton disappears. The concomitant oscillating structure in the redshift direction also disappears with decrease in C. The spectrum of bright solitons with a blueshift trend almost loses the trend under the negative chirped dark solitons. The entire spectrum is mainly divided into two parts. There is a peak at 1550 nm and another peak at 1560 nm. When C decreases, the peak value at 1560 nm gradually decreases and shortens the existing distance. Therefore, when the accompanying dark soliton is negatively chirped, the shape of the spectrum is optimized and the bright soliton spectrum is closer to the input spectrum.

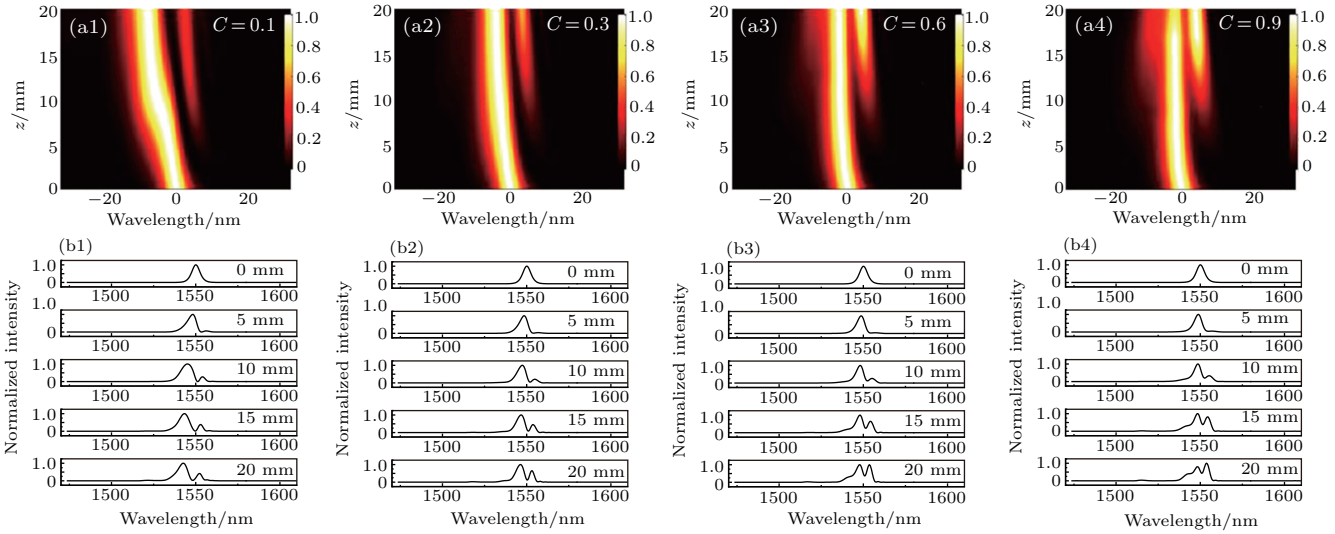


Fig. 5. (a) Spectral evolution of bright solitons when the chirp value of dark solitons is varied. (b) Spectrum of bright solitons at different transmission distances. (a1) and (b1) $C = 0.1$, (a2) and (b2) $C = 0.3$, (a3) and (b3) $C = 0.6$, and (a4) and (b4) $C = 0.9$.

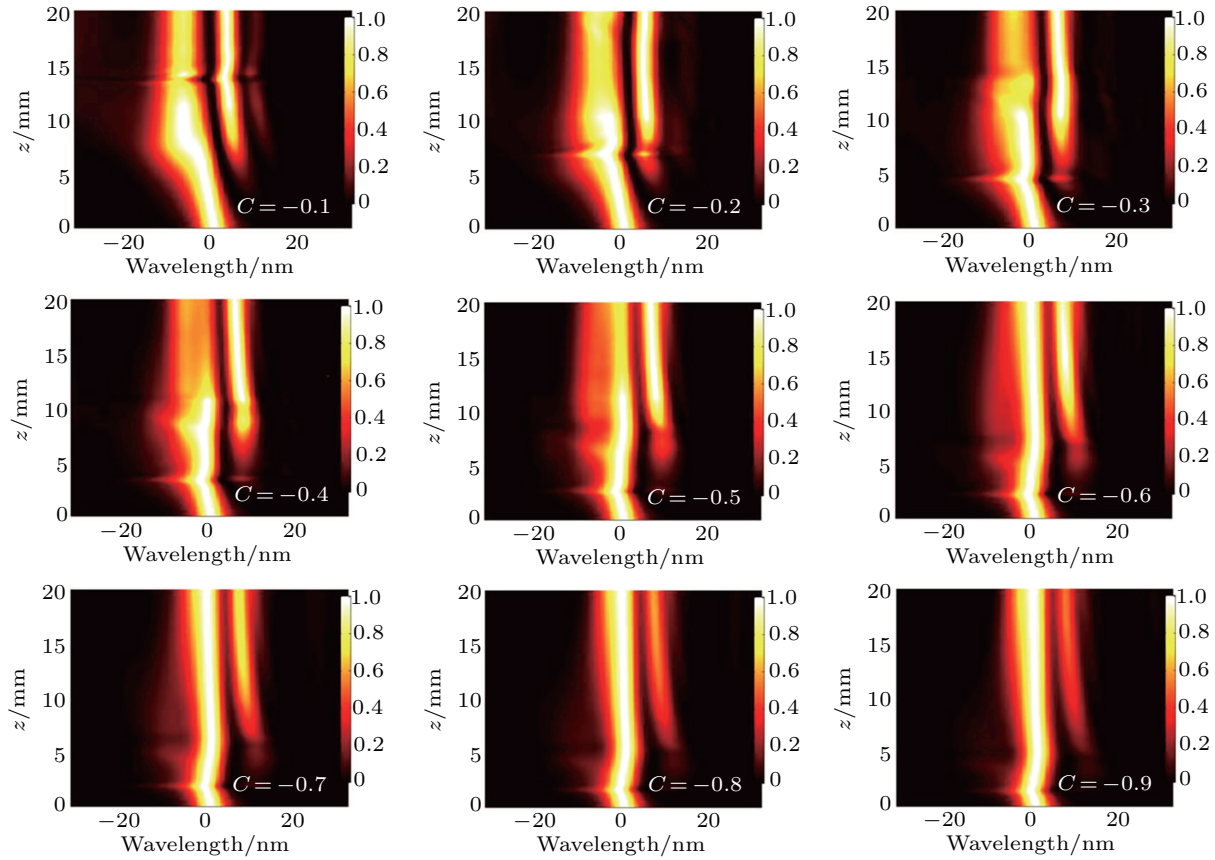


Fig. 6. Spectral evolution of bright soliton when the dark soliton is chirped with different negative chirps.

3.3. Effect of dispersion

In the transmission process, the fundamental-order soliton is subjected to dispersion perturbation in the nonlinear medium and generates dispersive wave.[10] Therefore, the "blue-shifted" dispersive wave is formed to create a supercontinuum spectrum.[11] For investigating the effect of dark soliton dispersion on the bright soliton spectrum, we modified the second-order dispersion of dark solitons in the normal dispersion region within the permissible range of material properties and simulated the spectral evolution of bright solitons.

According to Figs. 7(f) and 7(b), when $\beta_{2x} = 20$ ps^2/m, the bright soliton satisfies the phase matching condition and a spectral bulge is formed by dispersive wave radiation in the blueshift direction, and the spectral width is maximum. When the value of β_{2x} is reduced to 10 ps^2/m, the leftmost projection becomes insignificant, but the continuous spectral

structure on the left can still be observed in the evolution diagram (Fig. 7(a)). When β_{2x} is further increased, the continuous spectral structure on the left disappears, and the whole spectrum is blue-shifted with only two peaks at 1540 nm and 1550 nm. As shown in Figs. 7(c), 7(d), and 7(e), the peak at 1550 nm appears later and the peak value is decreased with the increase of β_{2x}. The accompanying oscillating structure in the redshift direction also disappears gradually, and the entire evolution diagram exhibits a redshift trend compared with the spectrum at $\beta_{2x} = 30$ ps^2/m. Therefore, the second-order dispersion of dark soliton affects the phase matching of bright soliton dispersion and the shape of bright soliton spectrum. It causes a redshift in the spectrum, compresses the spectral width, and makes the spectrum relatively steep.

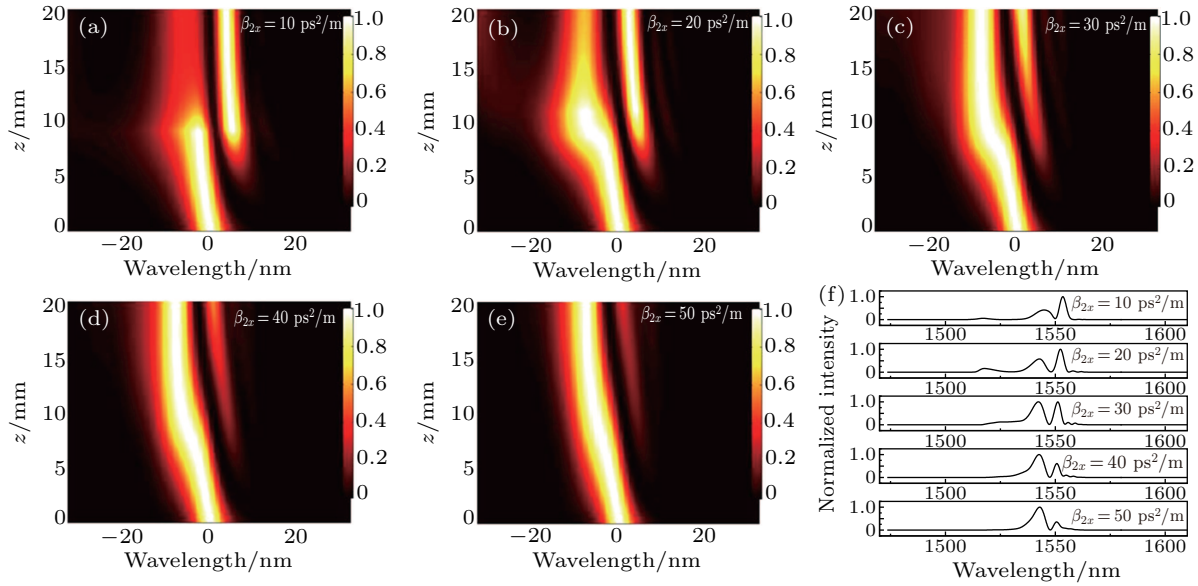


Fig. 7. (a)–(e) Spectral evolution diagram and (f) spectral line of the bright soliton when the second-order dispersion of the dark soliton is varied.

4. Conclusion

We proved that the behavior of the bright soliton transmitted alone in the ridged SOI optical waveguide is vastly different from that transmitted with the dark soliton. The main function of the dark soliton is to influence the splitting of soliton and to reduce the spectral width. If the power or energy of the dark soliton is increased, the energy of the bright soliton is affected, which in turn modifies the structure, width, and flatness of the spectrum. Further, the increase in the power of the bright soliton increases its splitting. When the energy of bright and dark solitons is high, the spectrum of bright soliton is no longer affected by the dark soliton. Both positively and negatively chirped dark solitons can promote the optimization of bright soliton spectra. Positive chirp effectively promotes the self-phase modulation and makes the spectrum symmetrical, while the negative chirp can promote the spectral evolution to the input spectrum. The dispersion of dark soliton affects the phase matching of bright soliton, influences the generation of dispersive wave radiation, increases the width of dark soliton dispersion compression spectrum, and broadens the bright soliton spectrum.

References

[1] Zhang Y W 1988 *Molecular Spectroscopy* (Beijing: University of Science and Technology of China Press) pp. 1–3
[2] Abrams K J, Dapor M, Stehling N and Azzolini M 2019 *Adv. Sci.* **6** 1900719
[3] Xie G H, Liu Y, Luo D P, Zhu Z W and Deng Z J 2019 *Chin. J. Nat.* **41** 15
[4] Diao G B and Diao L Q 2013 ZLCN 201320694966.0 [2013-11-06]
[5] Yang Z Y, *et al.* 2019 *Science* **365** 1017
[6] Reich G 2005 *Adv. Drug Deliver. Rev.* **57** 1109
[7] Chibireva L, Mazzolenia C, Voorta D, Borysowa J and Fink M 2018 *J. Nat. Gas Sci. Eng.* **55** 426
[8] Yin L H 2009 Ph. D. Dissertation (New York: University of Rochester)
[9] Dekker R, Usechak N, Forst M and Driessen A 2007 *J. Phy D: Appl. Phys.* **40** R249
[10] Dudly J M, Genty G and Goen S 2006 *Rev. Mod. Phys.* **78** 1135
[11] Austin D R, Sterke C M D, Eggleton B J and Brown T G 2006 *Opt. Express* **14** 11997
[12] Wen J 2015 *Nonlinear optical effect and application based on SOI waveguides.* Vol. 1 (Beijing: National Defense Industry Publishing) pp. 70–80
[13] Wang Y, Jia W G, Liu Z, Zhang J P and Neimule M 2019 *J. Mod. Opt.* **66** 1017
[14] Yin L H, Zhang J D, Fauchet P M and Agrawal G P 2009 *Opt. Lett.* **34** 476
[15] Chen R, Jia W G, Wang X Y, Zhang J P and Neimule M 2017 *J. Mod. Opt.* **64** 1809
[16] Chen R, Jia W G, Wang X Y and Lu J Q 2017 *J. Opt. Soc. Am. B* **34** 2295
[17] Wen J, Ma C J, Fan W and Fu H W 2015 *Opt. Laser Technol.* **71** 50
[18] Skryabin D V 2003 *Science* **301** 1705
[19] Yin L H, Lin Q and Agrawal G P 2007 *Opt. Lett.* **32** 391